HHS Public Access

Author manuscript

J Control Release. Author manuscript; available in PMC 2018 December 28.

Published in final edited form as:

J Control Release. 2017 December 28; 268: 416–426. doi:10.1016/j.jconrel.2017.10.019.

Ragweed pollen as an oral vaccine delivery system: Mechanistic insights

Md Jasim Uddin and **Harvinder Singh Gill***

Department of Chemical Engineering, Texas Tech University, Lubbock, TX 79409, USA

Abstract

We have recently developed pollen grains (PGs) as a unique method to deliver vaccines orally. Extensive chemical processing ensures allergen-free pollen microcapsules that can be loaded with vaccine antigens. Successful oral vaccine delivery has been previously demonstrated by us in a mouse model. However, the underlying mechanisms that help the processed PGs to achieve this goal were not fully understood. In this study, we wanted to understand the effects of chemically processed ragweed pollen (*Ambrosia elatior*) on the innate immune system. Intestinal epithelial cells, macrophages, and dendritic cells all bridge the innate and adaptive immunity. This study has shown that in response to ragweed pollen all these cells release inflammatory cytokines and chemokines. Scanning electron microscopy imaging revealed that macrophages can engulf ragweed pollen. In addition, in the presence of ragweed, mouse dendritic cells upregulated their activation markers, that is, CD40, CD80, CD86, and MHC class II molecules. Ragweed pollens did not cause significant cell membrane damage as compared to similarly sized poly (lactic-*co*-glycolic acid) particles. Moreover, ragweed did not affect the integrity of the intestinal epithelial cells. Ragweed pollens were also found in the subepithelial region of the small intestine 24 h after pollens were gavaged to mice. Our current findings lead to the conclusion that besides transporting the vaccine cargo, ragweed pollen shells have additional immunomodulatory properties that help the orally delivered antigen to effectively induce an immune response.

Keywords

Mucosal adjuvant; Oral vaccination; Persorption; Pollen phagocytosis; Pollen uptake; Ragweed pollen vaccine delivery

1. Introduction

Chemically processed pollen grains (PGs) have recently gained considerable attention due to their ability as an oral drug and vaccine carrier [1–5]. PGs are a microscopic body that contain the male reproductive cell (male gamete) of a plant [6]. A chemically resistant shell along with a coating on its surface known as ‘pollenkitt’ protects the gamete from harsh environmental conditions. The materials that reside inside the pollen shell or the pollenkitt

*Corresponding author at: Texas Tech University, Department of Chemical Engineering, 8th Street and Canton Ave, Mail Stop 3121, Lubbock, TX 79409-3121, USA. harvinder.gill@ttu.edu (H.S. Gill).

Conflict of interest disclosure

This potential conflict of interest has been disclosed and is managed by Texas Tech University.

may cause allergic reactions [7,8]. Thus, to ensure safety, these materials need to be removed before using pollen shells for oral vaccination. This can be achieved by treating PGs through a series of chemical treatments [1,9]. Empty pollen shells thus obtained can then be filled with vaccines of interest, and the acid resistant pollen shell [10] can protect the vaccine from gastric degradation. Using this concept our previous study performed in mice showed that pollen-based oral vaccination can induce long-lasting antigen-specific systemic and mucosal immune responses [1]. However, the mechanism by which PGs activate the immune system is unknown.

The small intestine is lined with intestinal epithelial cells (IECs). IECs provide protection from potentially invasive microorganisms by maintaining a physical and biochemical barrier [11]. The underlying subepithelial region is rich in immune cells including macrophages, dendritic cells (DCs), B cells, and T cells [12], which together help in maintaining gut immunity and tolerance [13]. It has been shown that IECs can secrete immunomodulatory factors at their basolateral surface leading to activation of these immune cells [14]. Therefore, IECs are an important component of the gut immunity. Since pollens are particulate in nature, they can directly interact with IECs and stimulate them. Furthermore, we have previously shown that pollens can translocate into the subepithelial region in mice [1]. Once in this region, they could directly interact with the resident antigen presenting cells (APCs). APCs such as macrophages and DCs phagocytose particles and release cytokines and chemokines that contribute to the functional polarization of T-cells [15,16]. Cytokines also contribute to the balance between immunity and tolerance. In addition, chemokines have a broad role in immune cell trafficking [17].

Hence, in this study, our objective was to evaluate the effect of pollen on IECs and to provide a systematic evaluation of the effect of pollen on macrophages and DCs. Morphologically and physiologically, the human colon epithelial cell line, Caco-2, closely resembles IECs. Therefore, it is widely used in oral drug permeability studies [18,19] and for characterizing different immunological functions of IECs, including cytokine release [20–22]. Accordingly, we selected Caco-2 cells to model IECs. We chose ragweed (RW) as a representative pollen and investigated their effect on Caco-2 monolayer integrity. We further evaluated the effect of RW pollen on mouse bone marrow derived macrophages (BMMs) and bone marrow derived dendritic cells (BMDCs) to better understand the mechanism of pollen-mediated oral vaccination.

2. Materials and methods

2.1. Pollens, chemicals, proteins and antibodies

Common ragweed (*Ambrosia elatior*) pollen was obtained from Pharmallerga (Lisov, Czech Republic). All chemicals and materials were purchased from Fisher Scientific (PA, USA) unless otherwise stated. Fluorescein isothiocyanate (FITC)-conjugated dextran (MW 4 kD and 40 kD), lipopolysaccharide (LPS) from *Escherichia coli* serotype O111:B4, and glutaraldehyde solution were purchased from Sigma-Aldrich (St. Louis, MO, USA). All cell culture reagents, lane marker reducing sample buffer, and Coomassie Brilliant Blue G-250 dye were purchased from Thermo Fisher Scientific (Waltham, MA, USA). Ovalbumin (OVA) was purchased from MP Biomedicals (Solon, OH, USA). Tris/Glycine/SDS

electrophoresis buffer, 4–20% mini-PROTEAN TGX precast gels for sodium dodecyl sulfate polyacrylamide gel electrophoresis (SDS-PAGE), and protein standards were obtained from Bio-Rad Laboratories, Inc. (Hercules, CA, USA). Purified mouse interferon gamma (IFN-γ), granulocyte-macrophage colony-stimulating factor (GM-CSF), and interleukin 4 (IL-4) proteins were purchased from eBioscience, Inc. (San Diego, CA, USA). Human 6-plex (IL-6, IL-8, monocyte chemoattractant protein-1 or MCP-1, GM-CSF, IL-1β, and tumor necrosis factor alpha or TNF-α) magnetic Luminex performance assay kit, individual human IL-6, IL-8 (CXCL-8), and MCP-1 (CCL-2) enzyme-linked immunosorbent assay (ELISA) kits, Mouse 8-plex (IL-4, IL-6, IL-10, IL-12p70, macrophage colony-stimulating factor or M-CSF, IL-1β, IFN-γ, and TNF-α) magnetic Luminex screening assay kits were bought from R&D systems, Inc. (Minneapolis, MN, USA). Purified anti-mouse CD16/32, allophycocyanin (APC)-conjugated anti-mouse CD11c, FITC-conjugated anti-mouse CD40, phycoerythrin (PE)-conjugated anti-mouse MHC II (I-A/I-E), APC/Cy7-conjugated anti-mouse CD86, APC-conjugated anti-mouse CD80 antibodies were purchased from Biolegend (San Diego, CA, USA).

2.2. Animals

Female, 6–8 week old BALB/c mice were obtained from Charles River Laboratories (Wilmington, MA, USA). Mice were maintained at Texas Tech University (TTU) Animal Care Service facility (TX, USA). All experiments were performed according to TTU Institutional Animal Care and Use Committee (IACUC) approved protocols.

2.3. Preparation of allergen-free RW shells

Naturally occurring potentially allergenic molecules were stripped from RW pollen shells by successive chemical treatments as described before [1]. Briefly, RW pollens were treated with acetone, 85% orthophosphoric acid, and potassium hydroxide. Between each chemical treatment pollens were filtered and washed with hot water, acetone, and 70% ethanol. Finally, pollens were dried at 60 °C until constant weight was achieved. RW pollens were stored at room temperature before use in the experiments.

For cell culture experiments, pollens were sterilized by incubating in 70% ethanol for 15 min followed by three washings with sterile water (soaking and vortexing pollen for 5 min in each washing step). Sterile pollens were resuspended in complete cell culture medium and stored at 4 °C until needed.

2.4. RW shell characterization

To investigate the interior of the pollen shells, samples of RW pollen were mixed with dry ice to make them brittle and manually cracked in a mortar and pestle. Samples were then coated with gold and palladium (Technics Hummer V sputter coater, Anatech USA, CA, USA). The morphology of the raw and processed RW was examined by a scanning electron microscope (SEM) (Hitachi S-4300 E/N FESEM, NY, USA). Elemental analysis using PerkinElmer 2400 Series II CHNS/O Analyzer (PerkinElmer, Inc., Waltham, MA, USA) was also performed to quantify the amount of nitrogen remaining in RW. Percent nitrogen obtained from sample analysis was then multiplied by a factor of 6.25 to convert it into percent protein [1]. All measurements were conducted in triplicate.

Chemically processed RW pollens suspended in phosphate buffered saline (PBS) were counted using hemocytometer and an automated cell counter (Countess II FL automated cell counter, Thermo Fisher Scientific, Waltham, MA, USA) to determine the number of pollens present per milligram of the sample.

2.5. Confocal microscopy

Chemically processed RW pollens were incubated with FITC-dextran solution (40 kD, 1 mg/ml in PBS) overnight at room temperature under vacuum (25 in. of Hg). Pollens were then carefully separated from the solution, mounted under a glass coverslip (#1.5) in Vectashield™ mounting medium (Vector Laboratories, Inc., Burlingame, CA, USA), and visualized with a laser scanning confocal microscope (Nikon Eclipse Ti-E, Nikon Instruments Inc., Melville, NY, USA). Images were captured by use of Nikon NIS-Elements AR software (version 4.13.01). A confocal microscope equipped with a 100× oil immersion objective (NA 1.4), and 488 and 561 nm lasers was used to image the RW.

2.6. SDS-PAGE

Raw or chemically processed RW pollens were heated with SDS-PAGE sample loading buffer (20 mg RW pollen/ml) at 95 °C for 10 min. Resulting solutions were then filtered using Vivaspin™ centrifugal concentrators (1000 kD MWCO, Sartorius AG, Goettingen, Germany) at 10,000 × *g* for 5 min at 4 °C.

To study OVA adsorption on RW surface, chemically processed pollens were incubated in OVA solution (5 mg RW per 500 μg OVA in 0.3 ml PBS) under vacuum. After overnight incubation, RW pollens were separated from the solution by centrifugal filtration. RW pollens were either dried (before washing group), or further washed three times with PBS, and then dried at 4 °C (after washing group). These dried RW pollens were then heated with sample loading buffer (20 mg RW pollen/ml) at 95 °C for 10 min to desorb the proteins. Pollens were then separated by centrifugal filtration and filtrates were analyzed.

SDS-PAGE analysis was performed by adding 20 μl of each sample to individual lanes of a 4–20% gradient gel and stained with Coomassie solution.

2.7. Cell culture, bone marrow derived macrophages and dendritic cells

Human colon epithelial cells Caco-2 (ATCC HTB 37), mouse peritoneal cavity monocyte/macrophage cells J774A.1 (ATCC TIB 67), mouse fibroblast cells L-929 (ATCC CCL-1), and Eagle's Minimum Essential Medium (EMEM) were purchased from American Type Culture Collection (ATCC, Manassas, VA, USA). J774A.1 cells were cultured in DMEM medium supplemented with 10% fetal bovine serum (FBS), 100 units/ml of penicillin, and 100 μg/ml of streptomycin. Caco-2 cells were cultured in EMEM medium supplemented with 10% FBS, 100 units/ml of penicillin, and 100 μg/ml of streptomycin. L-929 cells were used as a source of macrophage colony-stimulating factor (M-CSF) protein which is required to differentiate bone marrow cells into bone marrow derived macrophages (BMMs) [23]. L-929 cells were cultured in DMEM medium supplemented with 10% heat inactivated FBS, 10 mM HEPES, 1 mM sodium pyruvate, and 2–4 mM L-glutamine without antibiotics. Cells were plated in T75 flasks at a concentration of 5×10^5 cells/flask in 55 ml medium and

cultured at 37 °C and 5% CO_2 in an incubator for 13 days. Supernatants were collected after centrifugation at 200 ×*g* for 5 min at 4 °C, filtered using 0.22 μm filter, and stored at −80 °C until needed. The concentration of M-CSF in the supernatant was measured with ELISA using a commercially available kit (R&D systems, Inc.).

Bone marrow cells were harvested from tibia and femur of naïve mice ($n = 3$ mice) according to published protocols [24,25], and then differentiated into BMMs as per a previously published protocol [23]. Briefly, complete macrophage medium was made in DMEM supplemented with 10% heat inactivated FBS, 1 mM sodium pyruvate, 4 mM L-glutamine, 100 units/ml of penicillin, 100 μg/ml of streptomycin, 0.25 μg/ml of amphotericin B, and 150 ml of L-929 cell supernatant to make 500 ml of complete BMM differentiation medium. Bone marrow cells were cultured in a 150 mm non-treated cell culture dish at a concentration of 1.5×10^5 cells/ml with 25 ml medium. On day 3, 10 ml of fresh complete macrophage medium was added to each dish. On day 7, culture supernatants as well as non-adherent cells were removed and plates were washed with calcium and magnesium-free PBS. Adherent macrophage cells were removed with Cellstipper™, a non-enzymatic cell dissociation solution (Mediatech, Inc., Manassas, VA, USA), or by gentle scraping. Harvested BMMs were used for cytokine secretion study.

Differentiation of bone marrow cells into bone marrow derived dendritic cells (BMDCs) was performed according to published protocols [24,25]. Briefly, bone marrow cells were cultured in RPMI-1640 medium supplemented with 10% heat inactivated FBS, 1 mM sodium pyruvate, 2 mM L-glutamine, 55 μM 2-mercaptoethanol, 100 units/ml of penicillin, 100 μg/ml of streptomycin, 0.25 μg/ml of amphotericin B, 50 ng/ml of GM-CSF, and 50 ng/ml of IL-4 to differentiate into BMDCs. Cells were cultured in a 150 mm non-treated cell culture dish at a concentration of 2×10^5 cells/ml with 25 ml medium. On day 3, half of the medium was replaced with fresh BMDC differentiation medium. On day 6, one third of the medium was replaced with fresh BMDC differentiation medium. On day 7, loosely adherent and suspended BMDCs were harvested. Harvested BMDCs were used for cytokine secretion and flow cytometry study.

2.8. Measurement of Caco-2 monolayer transepithelial electrical resistance (TEER) and permeability

Caco-2 cells were seeded at a density of 2.5×10^5 cells per well in 12-well polyethylene terephthalate (PET) transwell filter inserts (0.4 μm pore size, Corning Incorporated, Corning, NY), and 700 μl and 1.5 ml medium was added to the apical and basolateral sides, respectively. Monolayers were grown for 22 days with growth medium changes every other day. TEER were measured before each medium change with Millicell ERS-2 meter (MilliporeSigma, Billerica, MA, USA) according to the manufacturer's instructions. Various concentrations of RW pollen were added to the apical side of the polarized cells for 24 h and TEER was measured every 2 h for 6 h. Caco-2 monolayers without RW were used as a negative control while 10 mM ethylene diamine tetra acetic acid (EDTA) treated cells were used as a positive control. EDTA was added only for the last 1 h (at 23rd h) of the experiment. TEER was also measured at 23 h and 24 h after RW addition. To determine if the presence of RW can affect electrical resistance of the insert, TEER of the insert without

cell monolayers but with culture medium alone or with various concentrations of RW were also measured. Average resistance of the inserts (without cells) was subtracted from the sample well to calculate the resistance of the cell monolayer and multiplied by the insert membrane area (0.9 cm^2). The following formula was used to calculate TEER:

$$\mathrm{TEER}_{\text{cell monolayer}} = (\mathrm{TEER}_{\text{sample}} - \mathrm{TEER}_{\text{insert}}) \times \text{insert membrane area}$$

FITC-dextran (MW 4 kD) is a commonly used paracellular marker for Caco-2 cell monolayers and has been previously used for permeability studies [18,19]. At the end of 24 h of TEER measurement, 1 mg/ml of FITC-dextran was added to the apical side of the cell monolayer. 200 μl of samples were collected from the basolateral compartment 2 h later. The intensity of FITC-dextran fluorescence was measured by a fluorescence spectrophotometer (Agilent Technologies, Santa Clara, CA, USA) at excitation/emission of 495/525 nm. All experiments were performed in triplicate.

2.9. Cytotoxicity assay

Cytotoxicity of RW pollen was determined by measuring the release of lactate dehydrogenase (LDH) into the Caco-2 culture medium. Caco-2 cells were seeded in a 96-well plate at a density of 1.5×10^4 cells/well in 100 μl medium for 24 h. The cells were next incubated with various concentrations of RW pollen or poly (lactic-*co*-glycolic acid) (PLGA) microparticles. PLGA particles of the same size as RW pollen (15 μm diameter, Phosphorex Inc., Hopkinton, MA, USA) were used for comparison purpose. After 6 h incubation with pollen or PLGA particles, cells were centrifuged at 200 × *g* for 5 min at room temperature to collect the supernatant. Supernatants were assayed using Pierce LDH cytotoxicity assay kit (Thermo Fisher Scientific, Waltham, MA, USA) according to the manufacturer's instructions to evaluate LDH concentration in the culture medium. To check if LDH can adsorb on the RW surface and produce an error in the assay, various concentrations of LDH standards (0.1–0.8 μl of LDH/ml of PBS) were incubated with RW (1 mg/ml) for 24 h at 37 °C. Supernatants were collected after spinning and LDH concentration was measured according to the above method. Percentage of cytotoxicity was calculated according to the published formula [26].

$$\%\,\mathrm{Cytotoxicity} = \left(\frac{\text{Absorbance of PLGA or RW treated cells} - \text{Absorbance of untreated cells}}{\text{Absorbance of completely lysed cells} - \text{Absorbance of untreated cells}}\right) \times 100$$

2.10. In vivo assessment of intestinal localization of RW pollen

Mice ($n = 3$) were fed 5 mg of processed RW pollen suspended in 0.3 ml of PBS via oral gavage using a 20G curved animal feeding needle (Cadence, Inc. Staunton, VA, USA). Another group of mice were gavaged only PBS without pollen. Mice were euthanized 24 h after feeding and their intestines were excised, longitudinally cut to expose the intestinal lumen, thoroughly washed with PBS to remove luminal contents, cut into small segments, and mounted on a glass slide with the intestinal epithelium facing towards the microscope

objective as described previously [1]. Samples were imaged using the confocal microscope equipped with 488 and 561 nm lasers.

2.11. Phagocytosis study

Mouse macrophage cells (J774A.1) were plated on a sterile glass coverslip at a concentration of 5×10^5 cells/ml in each well of a 6-well plate with 2 ml medium. After overnight cell attachment, sterile RW pollens (1 mg/ml) were added to each well to study phagocytosis. 24 h later cells were washed with PBS to remove unbound pollen and fixed with 2.5% glutaraldehyde solution for 40 min at room temperature. Cells were dehydrated with increasing concentrations of ethanol (50%, 70%, 80%, 90%, and 100%), dried using a critical point dryer (Balzers CPD 030, Balzers, Hudson, NH, USA), and coated with gold and palladium. Cells were then imaged with SEM. Images obtained from SEM were later processed and pseudo colored in Adobe Photoshop CS6 (San Jose, CA, USA) for better visualization [27,28].

2.12. Caco-2 cell cytokine release

Caco-2 cells were plated at a concentration of 1×10^6 cells/ml in each well of a 12 well plate and incubated overnight for attachment. Sterile RW pollens suspended in Caco-2 culture medium for 7–10 days were added at various concentrations and allowed to incubate for 24 h. Long-term incubation of RW in cell culture medium minimizes the adsorption of cell secreted protein on pollen surface and improves cytokine measurement accuracy and precision. Supernatants were collected after centrifugation at 200 × *g* for 5 min at 4 °C and stored at −80 °C until analyzed.

2.13. Cytokine secretion by primary BMMs and BMDCs

BMMs or BMDCs were cultured in RPMI-1640 medium supplemented with 10% heat inactivated FBS, 100 units/ml of penicillin, 100 μg/ml of streptomycin, and 0.25 μg/ml of amphotericin B. Cells were plated at a concentration of 1×10^6 cells/ml in each well of a 12-well plate and incubated overnight for attachment. Sterile RW pollens suspended in the cell culture medium were added at various concentrations and allowed to incubate for 24 h. As a positive control, BMMs were primed with 200 IU/ml of IFN-γ for 12 h followed by stimulation with 100 ng/ml of LPS for additional 12 h. 50 ng/ml of LPS was used as a positive control in the BMDC culture. Supernatants were collected after centrifugation at 200 ×*g* for 5 min at 4 °C and stored at −80 °C until analyzed with ELISA.

2.14. ELISA

Cytokines released by BMMs and BMDCs were quantified using mouse 8-plex (IL-4, IL-6, IL-10, IL-12p70, M-CSF, IL-1β, IFN-γ, and TNF-α) magnetic Luminex screening assay kits. Cytokines secreted by the Caco-2 cells were first screened with the human 6-plex (IL-6, IL-8, MCP-1, GM-CSF, IL-1β, and TNF-α) Luminex multiplex assay kit. Individual IL-6, IL-8, and MCP-1 sandwich ELISAs were subsequently used for the rest of the experiments. All ELISAs were performed according to the manufacturer's protocols in triplicate.

2.15. Flow cytometry to analyze BMDC activation

BMDCs were used to investigate whether RW pollen can activate DCs. BMDCs were cultured in a 150 mm dish at a concentration of 2×10^5 cells/ml (total 30 ml) and incubated overnight for attachment. RW pollens were then added at a concentration of 100 μg/ml and incubated for 48 h. Untreated cells were used as a negative control and 50 ng/ml LPS treated cells were used as a positive control. After 48 h cells were washed with calcium and magnesium-free PBS to remove unbound RW, and harvested using EDTA solution (5 mM EDTA, 10 min, 37 °C) for antibody labeling. Fcγ receptors on the cell surface were blocked with anti-mouse CD16/32 antibody, and then incubated with PE-conjugated anti-mouse MHC II mAb, FITC-conjugated anti-mouse CD40 mAb, APC-conjugated anti-mouse CD80 mAb, and APC/Cy7-conjugated anti-mouse CD86 mAb. 10,000 cells from each group were recorded using BD FACSAria II flow cytometer (BD Biosciences, San Jose, CA, USA) and analyzed in FlowJo V10 (FlowJo, LLC, Ashland, OR, USA). Autofluorescence from RW was distinguished from antibody bound fluorescent cells by their distinct forward and side scatter properties. APC-conjugated anti-mouse CD11c mAb was used to check the purity of the BMDCs.

2.16. Statistical analysis

All statistical analysis was performed using GraphPad Prism 6 (GraphPad Software, Inc., La Jolla, CA, USA). Two-tailed *t*-test was used to analyze elemental analysis data. One-way ANOVA with post hoc Tukey test was used for statistical calculations among all the groups in cytokine release experiments. Two-way ANOVA with post hoc Tukey test was used for statistical calculations in cytotoxicity experiments. Significance was considered for $p < 0.05$.

3. Results

3.1. Chemical treatment yields protein-free RW pollen

Raw RW pollens naturally contain several proteins that can trigger an allergic reaction in susceptible individuals [7,8]. Therefore, to remove these proteins from the RW shells, pollens were subjected to chemical treatment. After chemical treatment, RW pollens retain their spherical shape (diameter = 15 μm, Fig. 1A and C: unprocessed vs. 1B and D: chemically processed). Chemical processing also led to the opening of the aperture in the RW pollen wall (Fig. 1E vs. F). An aperture is a location in the pollen shell from where the pollen tube emerges during pollination [6]. An aperture is structurally different from the rest of the pollen wall and is weaker [6]. Opening of this aperture provides a pore (about 1 μm in diameter) through which the shell can be filled with proteins of interest. Chemical processing also removes native material from the inside of RW as shown by scanning electron micrographs of the hollow inner core (Fig. 1G: unprocessed vs. 1H: chemically processed). Two distinct shell layers are visible in both raw and processed RW, an outer layer (exine), and an inner layer (in-tine). Elemental analysis of processed RW pollens indicates that the protein content reduced from 25.8 ± 1.6% to 1.4 ± 0.2% (Fig. 2A). It should be noted that the pollen wall also contains nitrogen in its chemical building blocks [29]. However, since the molecular structure of the exine is not known, its contribution to nitrogen in elemental analysis is unclear. Thus, the amount, 1.4% protein, which is obtained by assuming that all of the nitrogen is emanating from residual proteins is a cautious

overestimate. Elemental analysis along with electron micrographs confirm that chemical treatment removes potential allergy-causing native pollen biomolecules.

3.2. Processed RW shells can be filled with large molecules

To determine the ability to fill RW pollen through the aperture, we used FITC-dextran (40 kD) as a model molecule. When vacuum was applied to RW suspended in an aqueous solution of FITC-dextran, air got removed from the pollen interior, and the resultant vacant space was then filled with the surrounding liquid. Empty RW (Figs. 2B and S1: Empty) shells show a fluorescent wall with a dark core. Upon application of vacuum the dark core became fluorescent indicating loading of FITC-dextran in the RW pollen (Figs. 2C and S1: FITC-dextran loaded).

3.3. OVA gets adsorbed on RW pollen surface

In addition to carrying antigen in encapsulated form, RW pollen can also transport the antigen in adsorbed form. Therefore, to assess the potential of protein adsorption on processed RW pollen, we performed SDS-PAGE analysis with OVA as a model vaccine-protein. First, RW pollen without OVA were characterized. We found that while raw RW pollens contain proteins ranging in molecular weights from 10 to 100 kD (Fig. 3: lane 2), processed RW showed no evidence of proteins (Fig. 3: lane 3). This demonstrates that chemical treatment fully removed native plant proteins from RW, making them safe for human use. Characterization of OVA solution showed presence of three protein bands (Fig. 3: lane 4). Commercial OVA (45 kD) contains small amounts of impurities from ovotransferrin (76 kD) and lysozyme (14.4 kD), which are the two abundant egg white proteins [30] and can explain the presence of these additional two bands. Characterization of RW pollens recovered from OVA solution after filtration (before washing group), showed presence of OVA (Fig. 3: lane 5). Interestingly, RW samples that were washed three times (after washing group) also showed the presence of OVA (Fig. 3: lane 6). Analysis of the three washings showed that the third and second washes did not contain any OVA (Fig. 3: lane 7,8), while the first wash contained OVA (Fig. 3: lane 9). This shows that OVA remains adsorbed on the pollen wall and it is not removed despite washing.

3.4. RW pollen does not impair Caco-2 cell monolayer integrity

RW pollen upon ingestion will come in direct contact with IECs. Therefore, we studied the effect of RW pollen on epithelial cell monolayer integrity. Caco-2 cells were selected as the model epithelial cell and grown on a porous surface to mimic the gut epithelium. The schematic of the experiment is illustrated in Fig. 4A. Monolayer development was confirmed by the high electrical resistance (> 485 $\Omega \cdot cm^2$) measured across all wells at day 22 (Fig. 4B). These TEER values were similar to those reported in other studies [19,31,32]. Various concentrations (0–2 mg/ml) of RW pollen were added to the apical side of the insert on day 22 and cultured for 24 h. To eliminate the possibility that addition of RW can change the TEER reading we performed a control study wherein just RW pollens were added to the inserts without Caco-2 cells. The result showed that RW pollens do not significantly increase or decrease the TEER reading ($p > 0.05$; Fig. S2). A fully established monolayer of Caco-2 cells had an average TEER value of 528 ± 27 $\Omega \cdot cm^2$ on day 22, which continued to rise during the 24 h culture period (Fig. 4C). Even after RW addition (0.5–2 mg), the TEER

continued to increase indicating that RW pollens do not affect Caco-2 monolayer integrity. Calcium chelators such as EDTA can cause calcium depletion, disrupt tight junctions, and cause loss of cell adhesion [33]. This, in turn, can increase transepithelial permeability and decrease TEER. Accordingly, we used EDTA as a positive control. Within 1 h of EDTA addition, TEER of cells decreased to zero (Fig. 4C) and showed the highest permeability for FITC-dextran across the cell layer (Fig. 4D). Thus, overall, RW pollen had an insignificant effect on Caco-2 cell TEER and permeability.

3.5. RW pollen are not cytotoxic to Caco-2 cells

After assessing monolayer integrity of Caco-2 cells, we investigated the cytotoxic profile of RW on Caco-2 cells. Various concentrations (0–1000 μg/ml, where 1 mg RW contains 1.64 ± 0.18 × 10^6 pollen particles) of RW pollen were cultured with Caco-2 cells (1.5 × 10^4 cells per well) for 6 h. The pollen to Caco-2 cell ratio was varied over a wide range from 0.1 to 10 to determine toxicity of RW pollens. PLGA particles have previously been shown to be safe for drug and vaccine delivery applications [34,35]. Thus, we used PLGA particles of a size similar to the RW as a comparative control. Low cell damage was seen when Caco-2 cells were cultured with up to 500 μg/ml of PLGA particles for 6 h (Fig. 5). At 1000 μg/ml, necrosis increased more than twofold for PLGA. No significant difference was found between PLGA and RW pollen in the studied concentration range ($p > 0.05$, two-way ANOVA). To eliminate the possibility that LDH could adsorb on RW and affect the assay, we incubated LDH at known concentrations with or without RW. We found that LDH concentration is not affected by the presence of RW pollens in the solution (Fig. S3).

3.6. RW pollen stimulate proinflammatory cytokines in Caco-2 cells

Upon ingestion, RW pollens will physically contact IECs, and this can stimulate IECs to secrete cytokines and chemokines that can further modulate the immune system. Therefore, in an in vitro setting, we quantified different inflammatory mediators secreted by Caco-2 cells upon incubation with RW pollens at different concentrations (0.5–5 mg/ml). Untreated cells were used as a negative control. Secretion of inflammatory cytokine (IL-6) and chemokines (IL-8 and MCP-1) significantly increased with increasing concentration of RW pollens (Fig. 6). However, GM-CSF, IL-1β, and TNF-α secretions were not observed during stimulation.

Interestingly, IL-8 and MCP-1 expression decreased at higher pollen concentration (4 mg/ml). We postulated that similar to OVA adsorption, other proteins may get adsorbed on to the pollen surface, and this adsorption may become substantial if RW pollen concentration becomes sufficiently high. To investigate this, known concentrations of IL-6, IL-8, and MCP-1 standards were incubated with or without 4 mg pollen for 24 h. It was found that the concentration of specific proteins in the supernatant decreased after 24 h of incubation with RW (Fig. S4). This shows that adsorption of IL-6, IL-8, and MCP-1 on to the RW surface can lead to drop in measurable values of these molecules in the supernatant.

3.7. RW pollen get internalized into the subepithelial region of mouse small intestine

RW pollen has a particulate nature, and like other particulate systems, they can get internalized into the mouse intestinal wall. Therefore, we examined the ability of RW pollen

to cross the intestinal epithelium barrier. Mice fed with chemically processed RW were euthanized 24 h after oral gavage, and their small intestines were imaged after washing. A schematic of the imaging technique is illustrated in Fig. 7A. Strong autofluorescence from RW pollen was utilized to locate them in different intestinal regions. Fig. 7B–D shows that RW can cross the intestinal epithelium and can be found in the subepithelial tissue, where they may establish a contact with epithelial as well as other innate immune cells. On the other hand, as expected, control mice (gavaged with only PBS) did not show any presence of pollen (Fig. 7E).

3.8. Interaction of RW pollen with macrophages and DCs

Since we saw RW pollen in the subepithelial region of the mouse intestine, we wanted to further characterize the interaction of RW with phagocytic cells and APCs that typically reside in these tissues. To study phagocytosis, mouse macrophage cells J774A.1 were cultured with RW pollen and imaged with an electron microscope. At the beginning of the incubation, all macrophage cells were on the bottom surface of the culture plate. However, 24 h later, macrophage cells could be seen migrating towards the top of RW pollen and spreading on their surface attempting to phagocytose them (Fig. 8A–D). Multiple cells were also seen attacking a single pollen (Fig. 8A). To determine whether macrophage cells were indeed being activated by RW pollen, we quantified different immune modulators secreted by macrophage cells. We used BMMs for this assay instead of J774A.1 cells to better represent the in vivo macrophage cell population. Results shown in Fig. 9A–B indicate that BMMs secrete proinflammatory cytokines (TNF-α and IL-1β) when cultured with RW at different concentrations (10–500 μg/ml). A significantly higher secretion of TNF-α was seen at 200 μg/ml and 500 μg/ml of RW, while IL-1β increased significantly at 500 μg/ml of RW.

DCs are professional APCs and are also found in the subepithelial region of the mouse intestine [13]. Therefore, we further characterized the effect of RW pollen on BMDCs. Similar to BMMs, BMDCs also secreted the proinflammatory cytokines TNF-α and IL-1β, but in addition secreted M-CSF (also known as Colony-stimulating factor-1 or CSF-1) and IL-6 (Fig. 9C–F). As with BMMs, a dose-dependent effect was also observed in BMDCs, with higher RW doses inducing significantly higher cytokine production. Expression of activation and maturation molecules on the surface of BMDCs was further analyzed by a flow cytometer. Untreated cells were used as a negative control while LPS treated cells were used as a positive control. Our analysis indicates that BMDCs cultured with chemically processed RW pollen showed an increase in the expression of CD40, CD80, CD86, and MHC class II molecules (Fig. 10). CD40 expression was absent in untreated cells (Fig. 10A) while both RW treated (Fig. 10B) and LPS treated (Fig. 10C) cells showed increased expression of CD40. Furthermore, both RW and LPS treatments upregulated the expression of CD80, CD86, and MHC class II molecules in BMDCs. Thus, RW treatment yielded mature BMDCs with higher expression of costimulatory molecules.

4. Discussion

We have previously seen that oral administration of pollens with the antigen helps to stimulate an antigen-specific systemic and mucosal immune response [1]. The objective of

this study was to understand how pollens help in this stimulation. To achieve this goal, we analyzed in vitro the interaction of RW pollen with IECs and APCs, specifically macrophages and DCs. To study the interaction of RW with IECs, we selected Caco-2 cells as a model human IEC cell line. We chose to study the interaction of RW pollen with macrophages and DCs because in our previous [1] and in this study we found that pollens localize in the subepithelial region, which is rich in APCs.

First, we verified that chemical treatment of RW pollen can completely remove proteins that are naturally found in RW. Removal of RW proteins from pollens is critical because they have been shown to cause allergy [7,8]. Protein removal was confirmed through elemental analysis and gel electrophoresis.

Analysis of RW pollens after chemical processing showed that their aperture was open. RW aperture is about 1 μm in diameter. This provides an opening through which pollen interior can be filled with different molecules. This is in contrast to lycopodium spores, which lack an aperture [1], but instead possess nanosized pores in their wall for passage of molecules. RW pollens were successfully filled with dextran solution as seen from confocal micrographs. The aperture in RW is a two-way path, it can allow molecules to move into the RW cavity, but at the same time, it can allow the encapsulated material to move out. However, even if the antigen was to leak out of the RW pollen, another way by which the vaccine antigen could get transported across the intestinal wall is through adsorption onto RW pollens. Indeed, using SDS-PAGE we did observe that OVA gets adsorbed onto RW pollens, and it stays adsorbed despite multiple washings. Furthermore, internalization of RW pollen into the subepithelial region within 24 h after pollen ingestion was verified in mice through use of confocal microscopy.

Similar to RW pollen, we have previously also observed lycopodium spores in the subepithelial space of mice intestine [1]. The exact mechanism by which pollens translocate across the IECs is not known and is worthy of future investigations. However, it is believed that this could occur by a process known as ‘persorption’. Persorption is a biophysical process by which paracellular translocation of large microparticles may happen in the gastrointestinal tract [36]. It has been suggested that persorption might occur through apoptotic epithelial cells [37]. Although uptake of larger particles is not widely studied, some reports have shown that particles measuring as much as 20 μm in diameter can get translocated across the epithelial barrier, albeit to a lesser extent as compared to smaller particles [38].

The interaction of RW pollens with epithelial cells could increase transepithelial permeability, which could then lead to higher antigen uptake and hence a better immune response. Therefore, we measured permeability across Caco-2 monolayers with or without incubation with RW. Neither did TEER across the Caco-2 monolayer change significantly nor did the influx of FITC-dextran increase when RW were added to Caco-2 cells. This suggests that RW pollens do not function as epithelial permeability enhancers. RW cytotoxicity on Caco-2 cells was also similar to that of PLGA microparticles. The cytotoxic effect seemed to increase with an increase in RW concentration, however this was not significant. Although we compared RW with an equal mass of similarly-sized PLGA

particles, there is still a difference in surface morphology and surface chemistry between the two. Furthermore, because RW has lower density than PLGA, the number of particles per mg of RW (1.6×10^6) was about five times higher than PLGA (3.1×10^5). Higher LDH release from RW treated cells might in part be due to these differences between RW pollens and PLGA particles. We also found that Caco-2 cells release IL-6, IL-8, and MCP-1 upon contact with RW pollen. IL-8 and MCP-1 are known to be potent recruiters and activators of neutrophils, monocytes, and macrophages [39.40]. MCP-1 is also associated with modulation of T cell responses towards Th2 type [40]. IL-6 induces B cell maturation into plasma cells and acts as a key survival factor for long-lived plasma cells [41]. Thus, RW interaction with IECs may provide an early signal for inflammatory response, leading to recruitment of more immune cells to the site.

Macrophages and DCs are professional APCs that play critical roles in antigen capture, processing, and presentation to the naïve T cells. Lamina propria of the small intestine harbors various subsets of APCs that can interact with orally delivered antigens and modulate immune responses [42,43]. Because we observed that RW pollen can translocate into the subepithelial region, we wanted to study how these cells interact with RW pollen. Macrophage cells are efficient in phagocytosis, and it is known that particle size, shape, surface charge, hydrophobicity, and surface chemistry affects phagocytosis [28,44,45]. It is also known that microparticles < 10 μm in diameter are more efficiently internalized by macrophages [44]. Thus, we wanted to study whether RW pollen, which has a diameter of 15 μm and has a unique microarchitecture on it's surface (instead of being smooth) can also be phagocytosed or not. Our results suggest that indeed RW can be phagocytosed by macrophages. Macrophages also secreted the proinflammatory cytokines TNF-α and IL-1β in the presence of RW pollens.

RW pollen also stimulated and activated BMDCs. RW at concentrations between 200 and 500 μg/ml induced significantly higher TNF-α, IL-1β, M-CSF, and IL-6 than the non-stimulated BMDCs. However, RW treated cells did not produce any IL-12p70, IFN-γ, or IL-10 (data not shown). While TNF-α, IL-1β, and IL-6 are proinflammatory cytokines, M-CSF has a broad biological effect on macrophage and DC activation and function [46]. CD40 was upregulated, which has several effector functions including activation of $CD4^+$ T cells, inducing expression of MHC class II on APCs, and B cell immunoglobulin class-switching [47]. MHC-II and the other costimulatory molecules (CD80 and CD86) were also upregulated, and these play a critical role in antigen presentation and $CD4^+$ T cell activation. Thus, upregulation of these molecules shows a possible role of RW shell as a DC activator.

How chemically processed RW pollens activate macrophages, DCs, and Caco-2 cells is not understood. The extensive chemical processing that RW pollens undergo removes free molecules. Thus, chemical moieties that are a covalent part of the pollen wall are likely to induce this stimulation and activation. However, the exact molecular structure of sporopollenin (outer wall) is not known. It is thought to comprise of oxygenated aromatics and aliphatics including phenols such as p-coumaric acid [29]. In addition, the inner wall has cellulosic composition [48]. These components of pollen wall may be recognized by pattern-recognition receptors (PRRs) in the APCs [49]. For example, macrophages express various carbohydrate-binding receptors such as C-type lectins, mannose receptor, or β-glucan

receptor [50]. These receptors have specificities for the carbohydrate groups that may be present in the exine of the RW. It was also demonstrated previously that carbohydrates can activate Caco-2 cells via engaging PRRs [32]. Thus, activation of Caco-2, BMMs, and BMDCs by RW may involve receptor-mediated events. Additional studies are required to further elucidate this mechanism.

Considering the above findings, we propose that chemically processed RW pollen interact with epithelial cells after oral ingestion, and stimulate them to secrete inflammatory cytokines. These cytokines can recruit innate immune cells to the basal subepithelial region, increasing the population of immune cells locally. Subsequently, some RW pollens are also translocated into the subepithelial region. In the subepithelial region pollens directly interact with innate immune cells such as macrophages and DCs. This pollen interaction can initiate a cascade of inflammatory responses, and cause activation of macrophages and DCs, and their maturation. The antigen carried in the RW pollen or that which is adsorbed on the RW pollen can be processed by these APCs leading to an adaptive immune response (Fig. 11).

5. Conclusion

Our studies have shown that chemically processed RW pollen do not compromise intestinal epithelial monolayer integrity. This is evident from the preservation of TEER of Caco-2 cell cultures and absence of cell membrane damage after the addition of RW pollen. Interaction of RW with Caco-2 cells induces the release of proinflammatory cytokines and chemokines. RW pollen can be phagocytosed by macrophage cells. This phagocytosis leads to the release of proinflammatory cytokines in a dose dependent manner. RW pollens also activate dendritic cells and lead to upregulation of maturation molecules on their surface.

This study answered some of the key questions related to the ability of RW pollen shells to activate the innate immune system. However, at the same time, it stimulates more questions. The molecular basis of RW interaction with the innate immune cells leading to secretion of proinflammatory cytokines needs more investigation. The exact mechanism of how RW pollen are internalized is still unknown. We hope that future research will shed light on these important questions and facilitate the use of this novel biomaterial for the development of an oral vaccine.

Supplementary Material

Refer to Web version on PubMed Central for supplementary material.

Acknowledgments

We thank Dr. Peter Keyel in the Department of Biological Sciences at Texas Tech university for his advice on primary macrophage culture. This research was supported by the National Institutes of Health (NIH) [grant number DP2HD075691] and the Defense Advanced Research Projects Agency (DARPA) [grant number N66001-12-1-4251]. HSG is a co-inventor on a patent related to the development of pollen grains for oral vaccines.

References

1. Atwe SU, Ma Y, Gill HS. Pollen grains for oral vaccination. J Control Release. 2014; 194:45–52. [PubMed: 25151980]

2. Diego-Taboada A, Beckett ST, Atkin SL, Mackenzie G. Hollow pollen shells to enhance drug delivery. Pharmaceutics. 2014; 6:80–96. [PubMed: 24638098]
3. Alshehri SM, Al-Lohedan HA, Chaudhary AA, Al-Farraj E, Alhokbany N, Issa Z, Alhousine S, Ahamad T. Delivery of ibuprofen by natural macroporous sporopollenin exine capsules extracted from *Phoenix dactylifera* L. Eur J Pharm Sci. 2016; 88:158–165. [PubMed: 26872877]
4. Lorch M, Thomasson MJ, Diego-Taboada A, Barrier S, Atkin SL, Mackenzie G, Archibald SJ. MRI contrast agent delivery using spore capsules: controlled release in blood plasma. Chem Commun. 2009:6442–6444.
5. Barrier S, Rigby AS, Diego-Taboada A, Thomasson MJ, Mackenzie G, Atkin SL. Sporopollenin exines: a novel natural taste masking material. LWT - Food Sci Technol. 2010; 43:73–76.
6. Edlund AF, Swanson R, Preuss D. Pollen and stigma structure and function: the role of diversity in pollination. Plant Cell. 2004; 16(Suppl):S84–S97. [PubMed: 15075396]
7. Wopfner N, Gadermaier G, Egger M, Asero R, Ebner C, Jahn-Schmid B, Ferreira F. The spectrum of allergens in ragweed and mugwort pollen. Int Arch Allergy Imm. 2005; 138:337–346.
8. Bordas-Le Floch V, Groeme R, Chabre H, Baron-Bodo V, Nony E, Mascarell L, Moingeon P. New insights into ragweed pollen allergens. Curr Allergy Asthm R. 2015; 15:63.
9. Mundargi RC, Potroz MG, Park JH, Seo J, Lee JH, Cho NJ. Extraction of sporopollenin exine capsules from sunflower pollen grains. RSC Adv. 2016; 6:16533–16539.
10. Diego-Taboada A, Maillet L, Banoub JH, Lorch M, Rigby AS, Boa AN, Atkin SL, Mackenzie G. Protein free microcapsules obtained from plant spores as a model for drug delivery: ibuprofen encapsulation, release and taste masking. J Mater Chem B. 2013; 1:707–713.
11. Peterson LW, Artis D. Intestinal epithelial cells: regulators of barrier function and immune homeostasis. Nat Rev Immunol. 2014; 14:141–153. [PubMed: 24566914]
12. Shakya AK, Chowdhury MYE, Tao W, Gill HS. Mucosal vaccine delivery: current state and a pediatric perspective. J Control Release. 2016; 240:394–413. [PubMed: 26860287]
13. Mowat AM. Anatomical basis of tolerance and immunity to intestinal antigens. Nat Rev Immunol. 2003; 3:331–341. [PubMed: 12669023]
14. Freytag LC, Clements JD. Mucosal adjuvants. Vaccine. 2005; 23:1804–1813. [PubMed: 15734046]
15. Arango Duque G, Descoteaux A. Macrophage cytokines: involvement in immunity and infectious diseases. Front Immunol. 2014; 5:491. [PubMed: 25339958]
16. Kapsenberg ML. Dendritic-cell control of pathogen-driven T-cell polarization. Nat Rev Immunol. 2003; 3:984–993. [PubMed: 14647480]
17. Griffith JW, Sokol CL, Luster AD. Chemokines and chemokine receptors: positioning cells for host defense and immunity. Annu Rev Immunol. 2014; 32:659–702. [PubMed: 24655300]
18. Kowapradit J, Opanasopit P, Ngawhirunpat T, Apirakaramwong A, Rojanarata T, Ruktanonchai U, Sajomsang W. In vitro permeability enhancement in intestinal epithelial cells (Caco-2) monolayer of water soluble quaternary ammonium chitosan derivatives. AAPS Pharm Sci Tech. 2010; 11:497–508.
19. Cox DS, Raje S, Gao H, Salama NN, Eddington ND. Enhanced permeability of molecular weight markers and poorly bioavailable compounds across Caco-2 cell monolayers using the absorption enhancer, zonula occludens toxin. Pharm Res. 2002; 19:1680–1688. [PubMed: 12458674]
20. Jung HC, Eckmann L, Yang SK, Panja A, Fierer J, Morzycka-Wroblewska E, Kagnoff MF. A distinct array of proinflammatory cytokines is expressed in human colon epithelial cells in response to bacterial invasion. J Clin Invest. 1995; 95:55–65. [PubMed: 7814646]
21. Eckmann L, Jung HC, Schurer-Maly C, Panja A, Morzycka-Wroblewska E, Kagnoff MF. Differential cytokine expression by human intestinal epithelial cell lines: regulated expression of interleukin 8. Gastroenterology. 1993; 105:1689–1697. [PubMed: 8253345]
22. Stadnyk AW. Intestinal epithelial cells as a source of inflammatory cytokines and chemokines. Can J Gastroenterol. 2002; 16:241–246. [PubMed: 11981577]
23. Zhang X, Goncalves R, Mosser DM. The isolation and characterization of murine macrophages. Curr Protoc Immunol. 2008; 14(11):11–14.11.14.
24. Boudreau J, Koshy S, Cummings D, Wan Y. Culture of myeloid dendritic cells from bone marrow precursors. J Vis Exp. 2008:e769.

25. Lutz MB, Kukutsch N, Ogilvie ALJ, Rossner S, Koch F, Romani N, Schuler G. An advanced culture method for generating large quantities of highly pure dendritic cells from mouse bone marrow. J Immunol Methods. 1999; 223:77–92. [PubMed: 10037236]
26. Chan FKM, Moriwaki K, De Rosa MJ. Detection of necrosis by release of lactate dehydrogenase activity. Methods Mol Biol. 2013; 979:65–70. [PubMed: 23397389]
27. Lu Z, Qiao Y, Zheng XT, Chan-Park MB, Li CM. Effect of particle shape on phagocytosis of CdTe quantum dot-cystine composites. Medchemcomm. 2010; 1:84–86.
28. Champion JA, Mitragotri S. Role of target geometry in phagocytosis. Proc Natl Acad Sci USA. 2006; 103:4930–4934. [PubMed: 16549762]
29. Descolas-Gros C, Schölzel C. Stable isotope ratios of carbon and nitrogen in pollen grains in order to characterize plant functional groups and photosynthetic pathway types. New Phytol. 2007; 176:390–401. [PubMed: 17888118]
30. Abeyrathne EDNS, Lee HY, Ahn DU. Egg white proteins and their potential use in food processing or as nutraceutical and pharmaceutical agents—A review. Poult Sci. 2013; 92:3292–3299. [PubMed: 24235241]
31. Cox DS, Gao H, Raje S, Scott KR, Eddington ND. Enhancing the permeation of marker compounds and enaminone anticonvulsants across Caco-2 monolayers by modulating tight junctions using zonula occludens toxin. Eur J Pharm Biopharm. 2001; 52:145–150. [PubMed: 11522479]
32. De Smet R, Demoor T, Verschuere S, Dullaers M, Ostroff GR, Leclercq G, Allais L, Pilette C, Dierendonck M, De Geest BG, Cuvelier CA. β-Glucan microparticles are good candidates for mucosal antigen delivery in oral vaccination. J Control Release. 2013; 172:671–678. [PubMed: 24041710]
33. Tomita M, Hayashi M, Awazu S. Absorption-enhancing mechanism of EDTA, Caprate, and Decanoylcarnitine in Caco-2 cells. J Pharm Sci. 1996; 85:608–611. [PubMed: 8773957]
34. Lin R, Shi Ng L, Wang C-H. In vitro study of anticancer drug doxorubicin in PLGA-based microparticles. Biomaterials. 2005; 26:4476–4485. [PubMed: 15701377]
35. Anderson JM, Shive MS. Biodegradation and biocompatibility of PLA and PLGA microspheres. Adv Drug Deliv Rev. 1997; 28:5–24. [PubMed: 10837562]
36. Volkheimer G, Schulz FH. Persorption of vegetable food particles. Qual Plant Mater Veg. 1968; 17:17–30.
37. Yuji M, Fujimoto M, Miyata H, Inamoto T, Qi WM, Yamamoto K, Warita K, Yokoyama T, Hoshi N, Kitagawa H. Persorption mechanisms of luminal antigenic particulates via apoptotic epithelial cells of intestinal villi into systemic blood circulation in orally immunized rats. J Vet Med Sci. 2007; 69:339–346. [PubMed: 17485920]
38. Carr KE, Hazzard RA, Reid S, Hodges GM. The effect of size on uptake of orally administered latex microparticles in the small intestine and transport to mesenteric lymph nodes. Pharm Res. 1996; 13:1205–1209. [PubMed: 8865313]
39. Baggiolini M, Clark-Lewis I. Interleukin-8, a chemotactic and inflammatory cytokine. FEBS Lett. 1992; 307:97–101. [PubMed: 1639201]
40. Deshmane SL, Kremlev S, Amini S, Sawaya BE. Monocyte chemoattractant protein-1 (MCP-1): an overview. J Interferon Cytokine Res. 2009; 29:313–326. [PubMed: 19441883]
41. Hunter CA, Jones SA. IL-6 as a keystone cytokine in health and disease. Nat Immunol. 2015; 16:448–457. [PubMed: 25898198]
42. Chang SY, Ko HJ, Kweon MN. Mucosal dendritic cells shape mucosal immunity. Exp Mol Med. 2014; 46:e84. [PubMed: 24626170]
43. Mowat AM, Agace WW. Regional specialization within the intestinal immune system. Nat Rev Immunol. 2014; 14:667–685. [PubMed: 25234148]
44. Champion JA, Walker A, Mitragotri S. Role of particle size in phagocytosis of polymeric microspheres. Pharm Res. 2008; 25:1815–1821. [PubMed: 18373181]
45. Thiele L, Merkle HP, Walter E. Phagocytosis and phagosomal fate of surface-modified microparticles in dendritic cells and macrophages. Pharm Res. 2003; 20:221–228. [PubMed: 12636160]

46. Chitu V, Stanley ER. Colony-stimulating factor-1 in immunity and inflammation. Curr Opin Immunol. 2006; 18:39–48. [PubMed: 16337366]
47. Grewal IS, Flavell RA. The role of CD40 ligand in costimulation and T-cell activation. Immunol Rev. 1996; 153:85–106. [PubMed: 9010720]
48. Jiang J, Zhang Z, Cao J. Pollen wall development: the associated enzymes and metabolic pathways. Plant Biol. 2013; 15:249–263. [PubMed: 23252839]
49. Akira S, Uematsu S, Takeuchi O. Pathogen recognition and innate immunity. Cell. 2006; 124:783–801. [PubMed: 16497588]
50. Aderem A, Underhill DM. Mechanisms of phagocytosis in macrophages. Annu Rev Immunol. 1999; 17:593–623. [PubMed: 10358769]

Appendix A. Supplementary data

Supplementary data to this article can be found online at https://doi.org/10.1016/j.jconrel.2017.10.019.

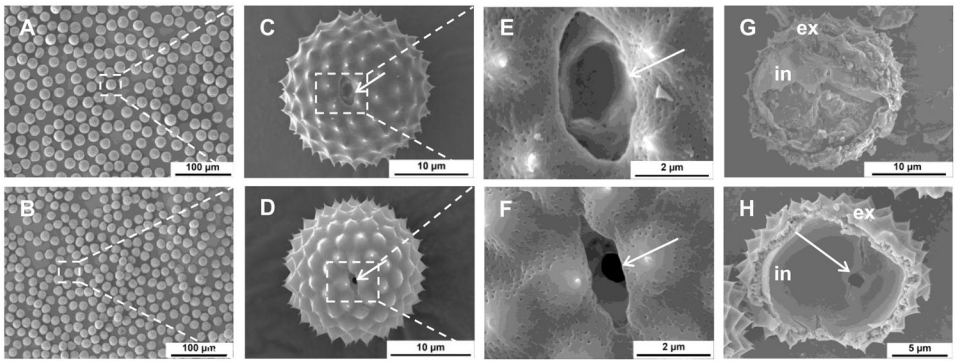

Fig. 1.

Scanning electron micrographs of ragweed (RW) pollen grains before and after chemical treatment. Low-magnification images of a collection of RW pollen (A) before and (B) after chemical treatment. High magnification images of a single RW pollen (C) before and (D) after chemical treatment. Magnified view of a RW aperture (indicated by arrow) (E) before and (F) after chemical treatment. Aperture gets opened after chemical processing. Images of manually cracked pollen interior (G) before and (H) after chemical treatment. An open aperture can be seen from the inside (arrow in H), ex = exine or outer layer, in = intine or inner layer.

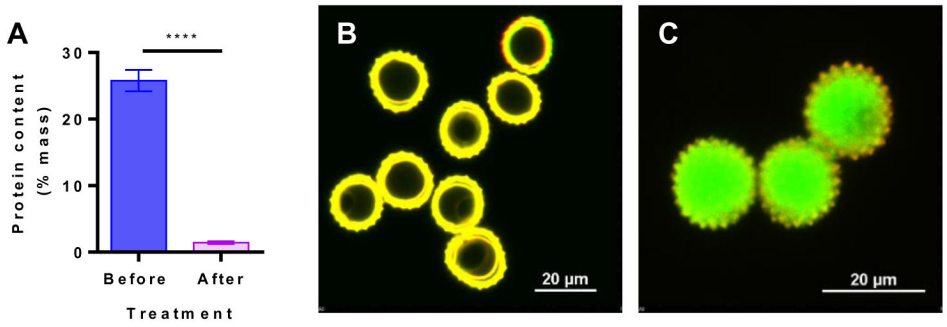

Fig. 2.

Characterization of ragweed (RW) pollen grains. (A) Elemental analysis of RW pollen showing a decrease in protein content after chemical treatment. Values shown are means ± SD for three independent experiments. $P \leq 0.0001$ [****]. Confocal micrographs (merged image from excitation with 488 and 561 nm lasers) for (B) empty chemically processed RW pollen shells showing strong auto fluorescence, and (C) chemically processed RW pollen shells filled with FITC-dextran (MW 40 kD) solution.

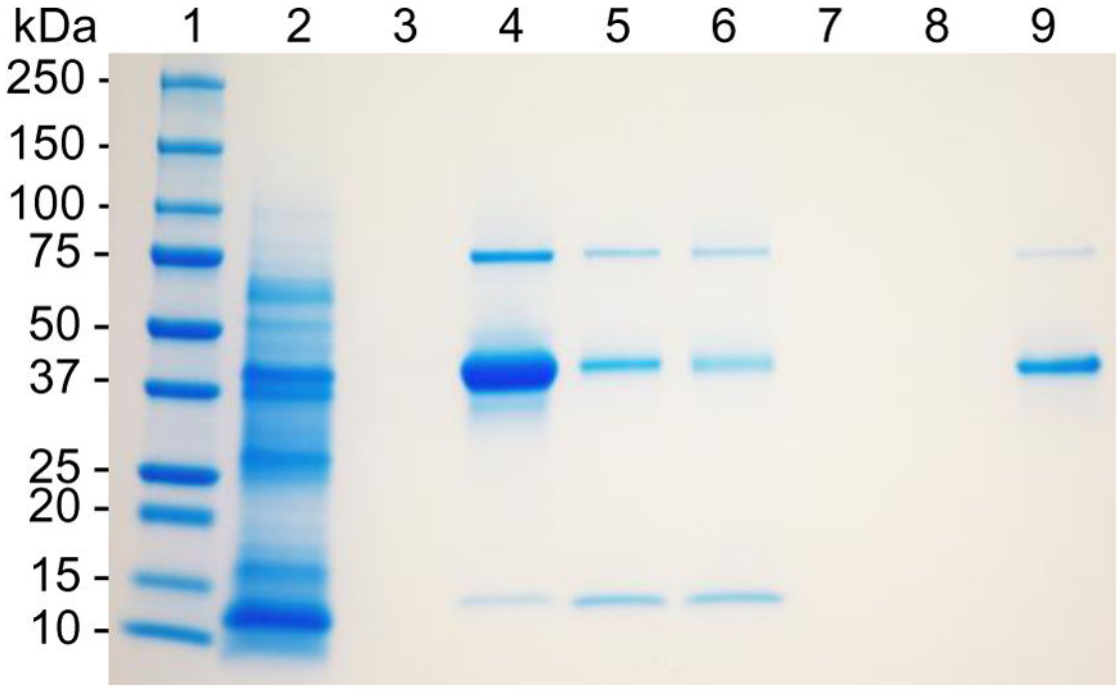

Fig. 3.

SDS-PAGE analysis revealing adsorption of OVA on ragweed (RW) surface. Lane 1: protein ladder; lane 2: extract of raw unprocessed RW pollen; lane 3: extract of chemically processed RW pollen; lane 4: OVA; lane 5: chemically processed RW pollen incubated with OVA, filtered and dried; lane 6: chemically processed RW pollen incubated with OVA, filtered, washed three times, and dried; lane 7: supernatant from the third wash; lane 8: supernatant from the second wash; lane 9: supernatant from the first wash. The gel image is representative of three independent experiments.

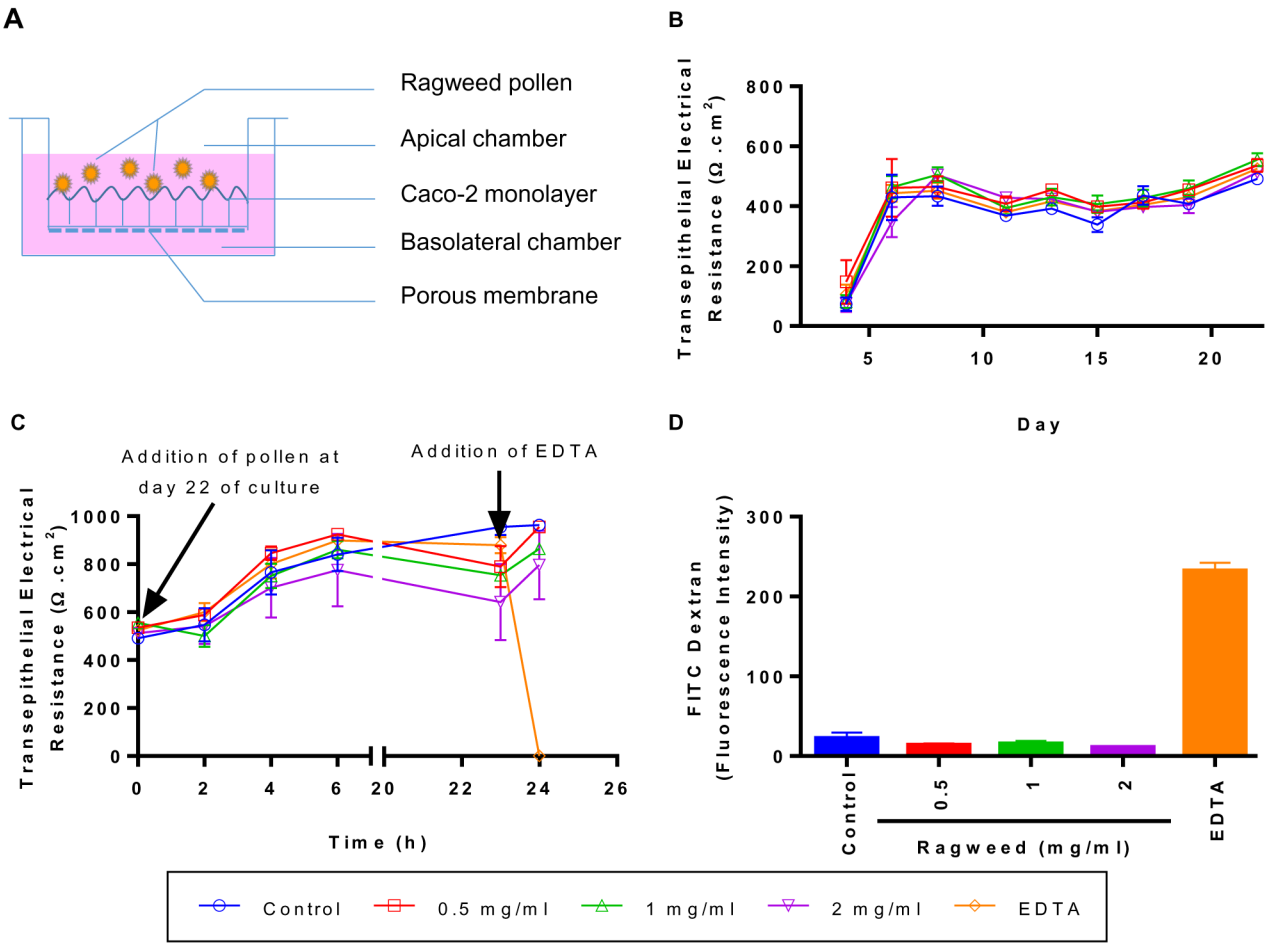

Fig. 4.

Transepithelial electrical resistance (TEER) and permeability of Caco-2 cells in the presence of chemically processed ragweed (RW) pollen. (A) Schematic of the experiment, (B) TEER values before the addition of RW pollen, (C) TEER values after the addition of RW pollen or EDTA, and (D) FITC-dextran (MW 4 kD) permeability across the Caco-2 monolayer. Values shown are means ± SD for three independent experiments.

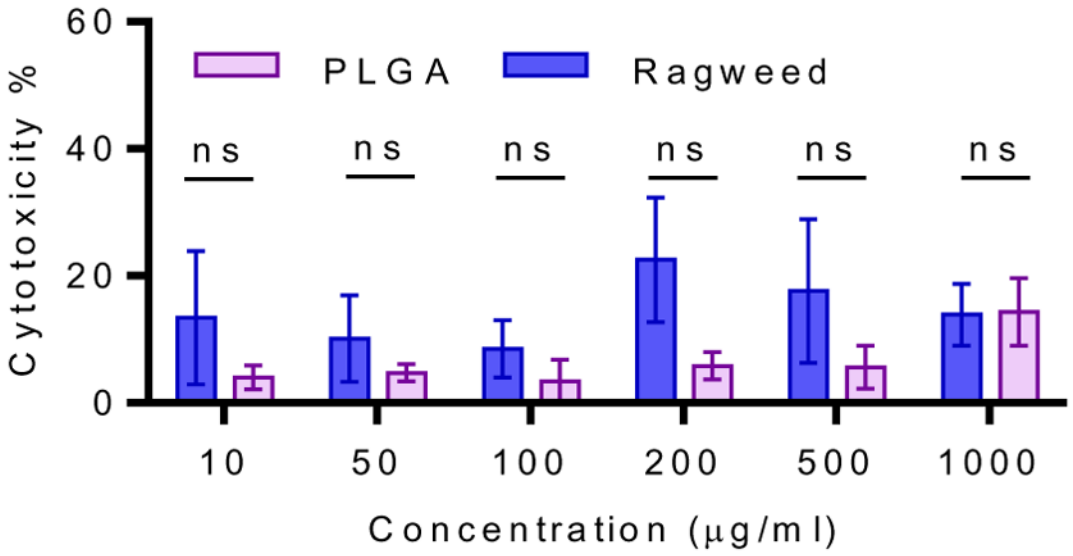

Fig. 5.

Cytotoxicity of ragweed (RW) pollen in comparison with poly(lactic-*co*-glycolic) acid (PLGA). Caco-2 cells were cultured with chemically processed RW pollen or 15 μm diameter PLGA particles for 6 h. Cell membrane damage was assessed with LDH assay. Values shown are means ± SD for three independent experiments. ns = not significant.

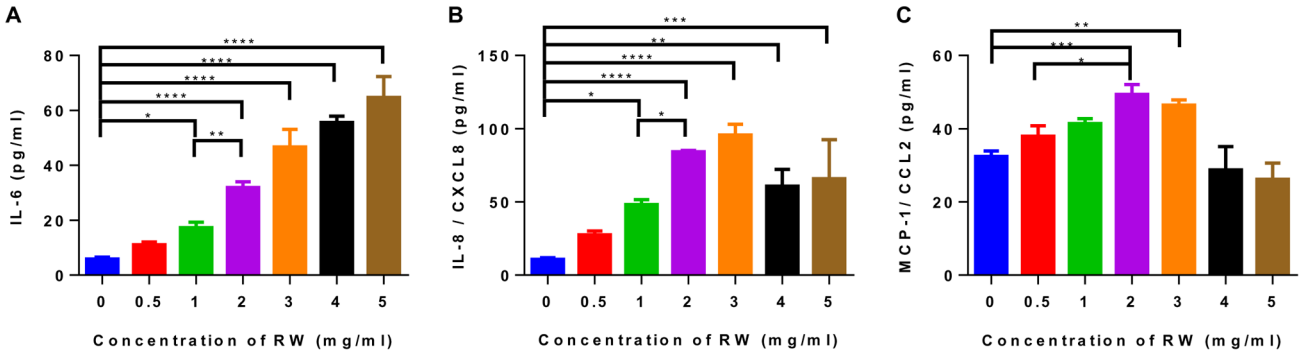

Fig. 6.

Cytokine secretion by Caco-2 cells in the presence of ragweed (RW) pollen. Caco-2 cells were cultured with different concentrations of chemically processed RW pollens for 24 h. Cytokines released from the cells were measured with ELISA. (A) IL-6, (B) IL-8, and (C) MCP-1 secretion stimulated by RW pollen. Values shown are means ± SD for three independent experiments. $P \leq 0.05$ [*], $P \leq 0.01$ [**], $P \leq 0.001$ [***], $P \leq 0.0001$ [****].

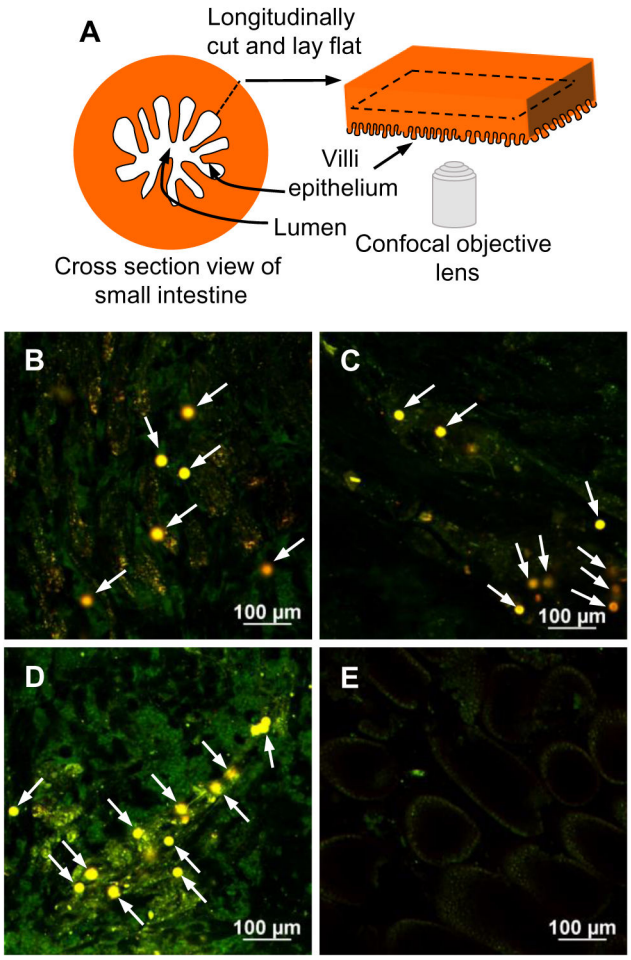

Fig. 7.

Internalization of ragweed (RW) pollen into subepithelial space of mouse small intestine. Mice were orally gavaged with 5 mg of chemically processed RW pollen or only PBS (control). Mouse small intestines were isolated after euthanasia, thoroughly washed, and imaged 24 h after oral gavage. (A) Schematic of the imaging method. Confocal micrographs of sections obtained from the (B) beginning, (C) middle, and (D) end regions of the small intestine of mice that were gavaged with RW pollen. Arrows point to the RW pollens. (E) Confocal micrograph of a small intestine section obtained from a control mouse that was gavaged only with PBS. The data is representative of three mice that were gavaged with RW pollens.

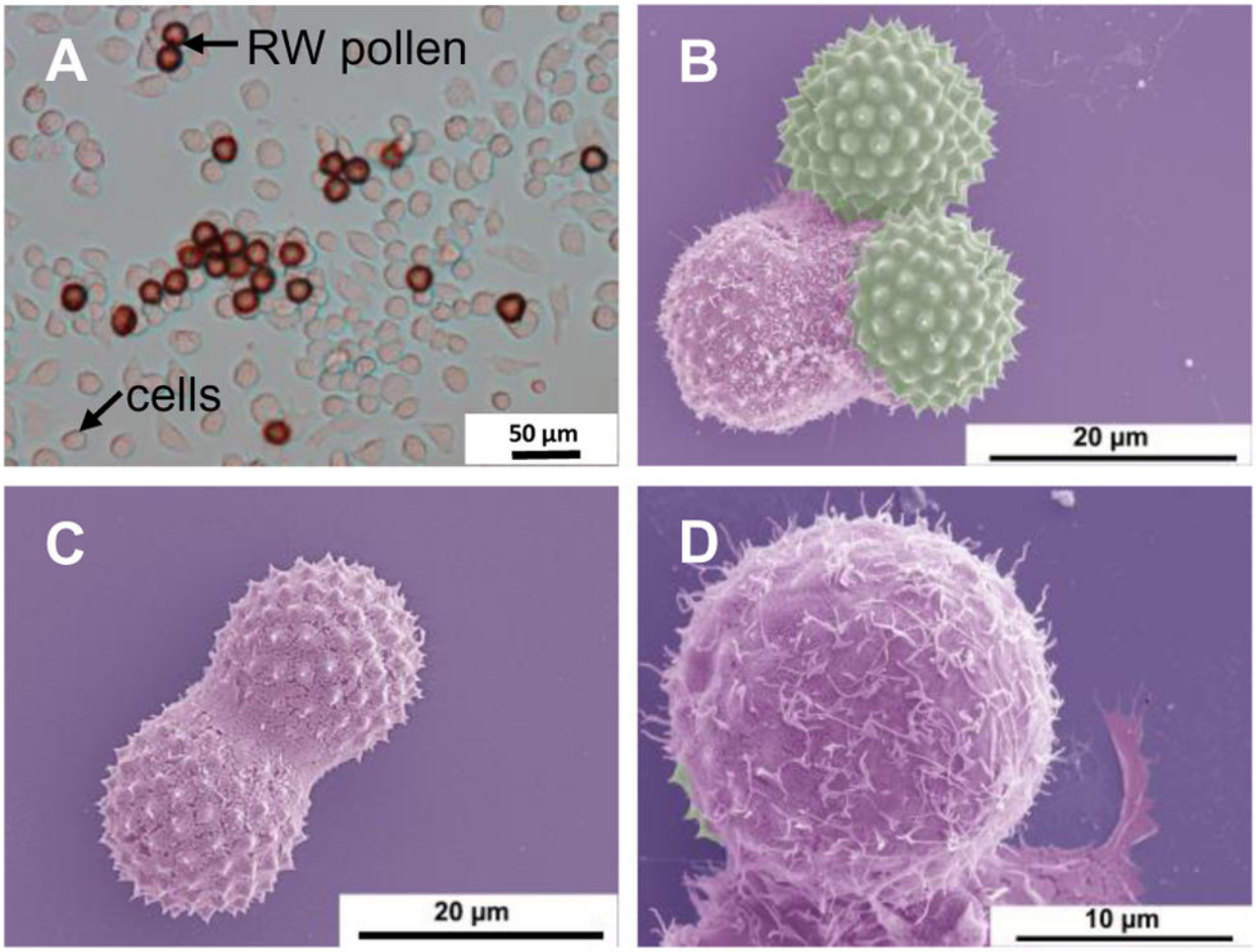

Fig. 8.

Phagocytosis of ragweed (RW) pollen by mouse macrophage cell (J774A.1). (A) Differential interference contrast (DIC) micrograph of RW pollens surrounded by multiple macrophage cells, (B) pseudo colored scanning electron micrograph of RW pollens being phagocytosed by a macrophage cell, (C) pseudo colored scanning electron micrograph showing a single macrophage spreading over two RW pollens, and (D) pseudo colored scanning electron micrograph at a higher magnification showing phagocytic interaction of a macrophage with RW pollen.

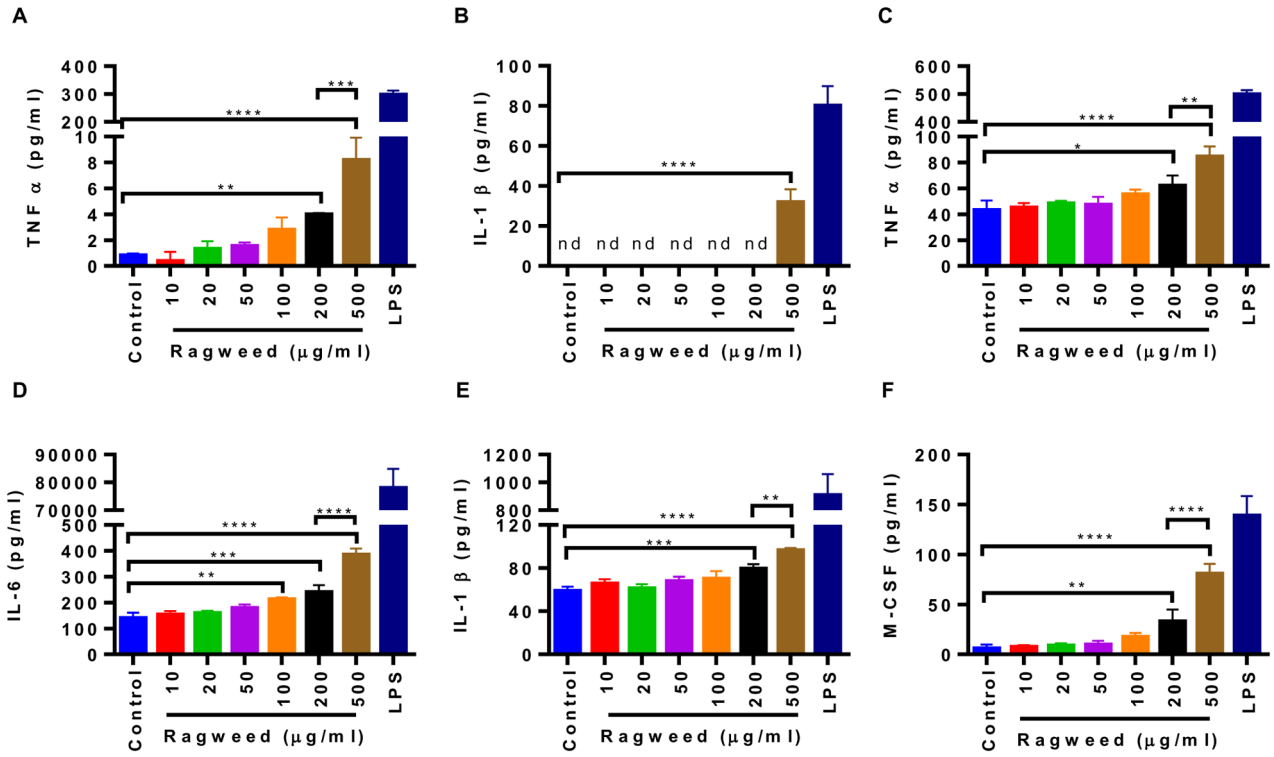

Fig. 9.

Cytokine production by mouse bone marrow derived macrophages (BMMs) and bone marrow derived dendritic cells (BMDCs) in the presence of ragweed (RW) pollen. Cells were cultured with different concentrations of chemically processed RW pollens for 24 h. (A–B) cytokines released by BMMs, (C–F) cytokines released by BMDCs. 100 and 50 ng/ml of LPS were used as a positive control for BMMs and BMDCs, respectively, while untreated cells were used as a negative control. Values shown are means ± SD for three independent experiments. $P \leq 0.05$ [*], $P \leq 0.01$ [**], $P \leq 0.001$ [***], $P \leq 0.0001$ [****], nd = not detectable. LPS treated positive controls were excluded from statistical analysis.

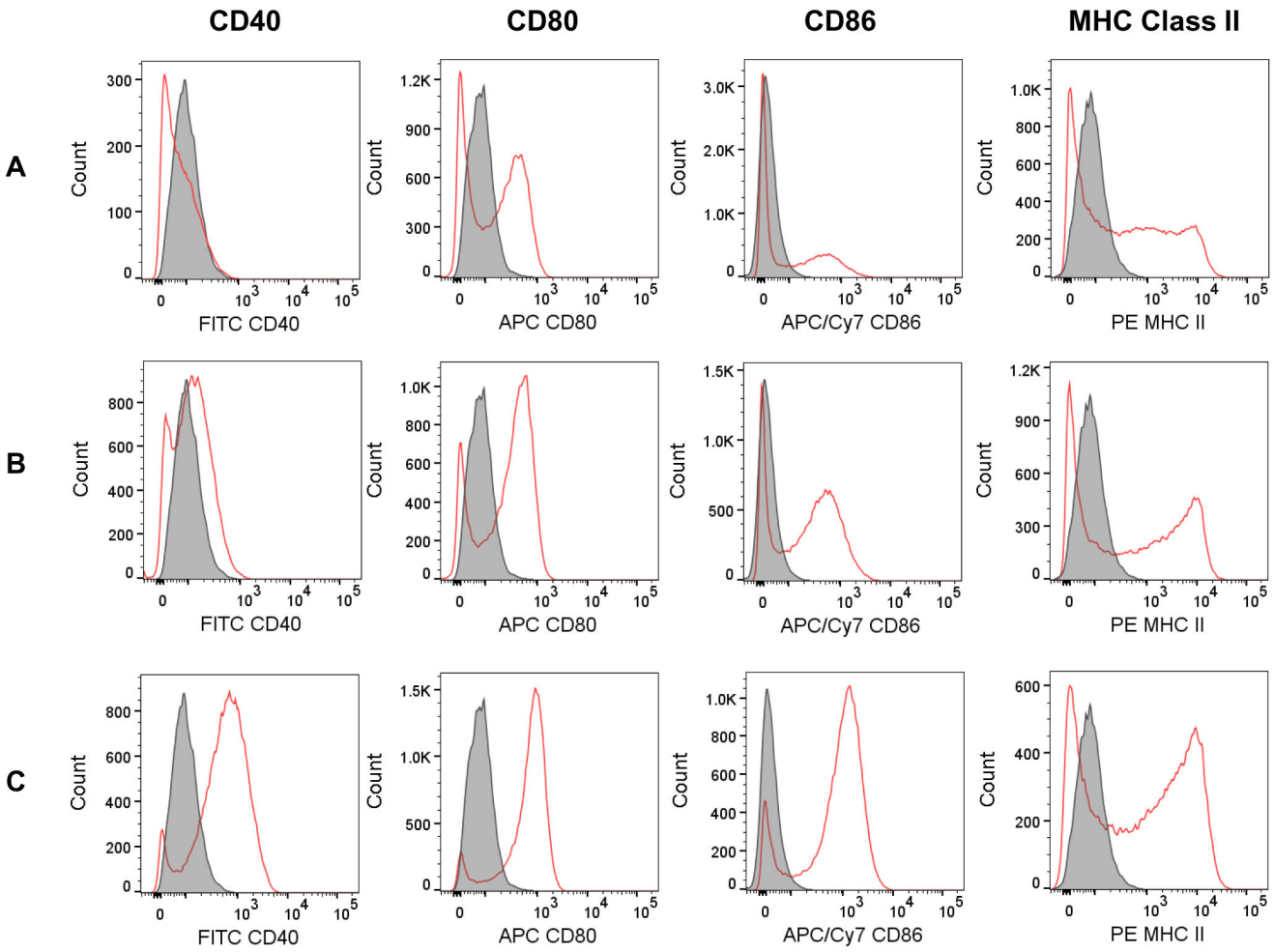

Fig. 10.

Cell surface expression of activation and maturation markers in bone marrow derived dendritic cells (BMDCs). Cells were cultured for 48 h either untreated or in the presence of chemically processed ragweed (RW) pollen or LPS. Expression of CD40, CD80, CD86, and MHC Class II on (A) untreated cells (control), (B) cells after treatment with 100 μg/ml of RW, and (C) cells after treatment with 50 ng/ml of LPS. Filled histogram represents unstained cells and open histogram represents antibody stained cells.

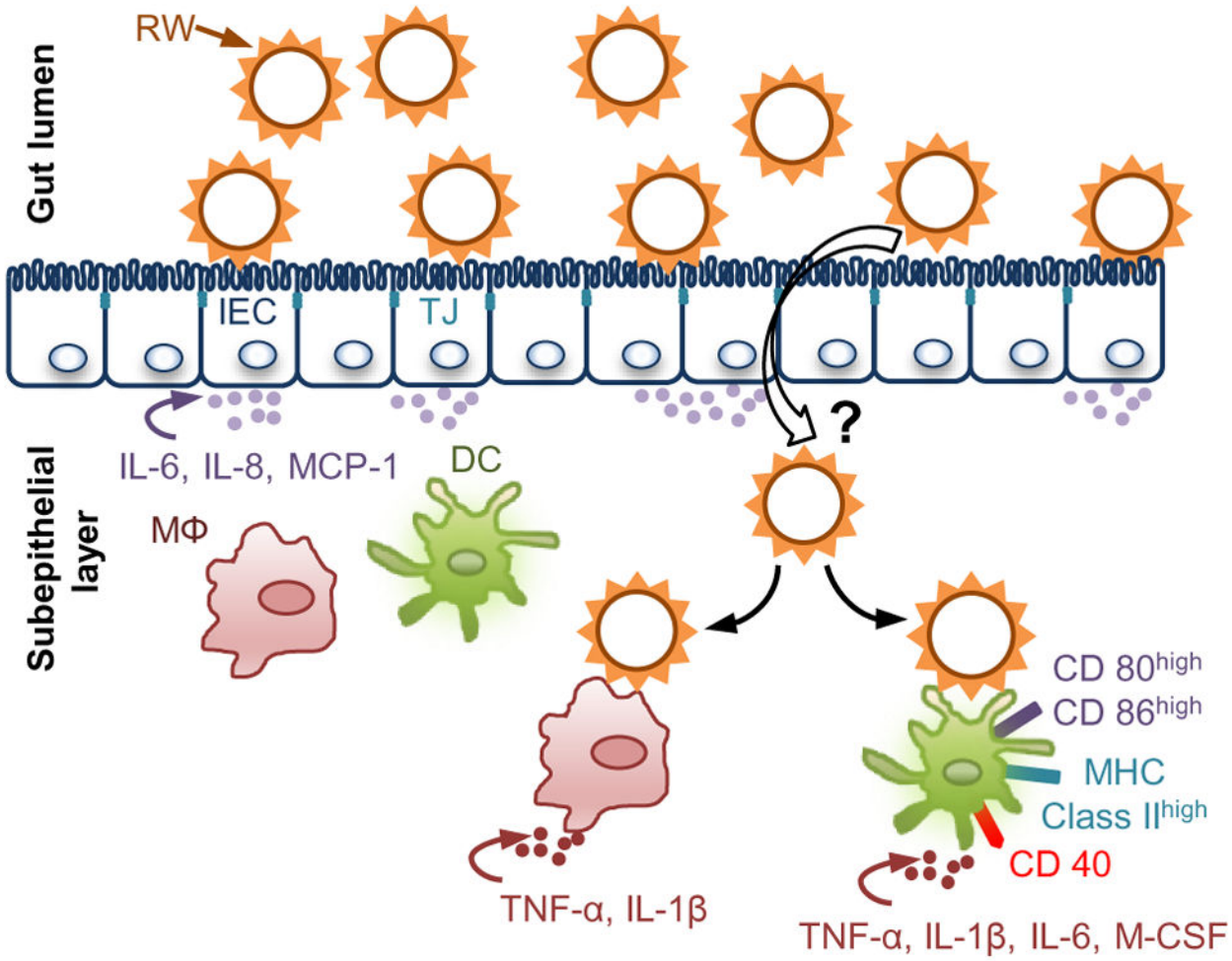

Fig. 11.

A proposed mechanism for pollen-based oral vaccination. After oral ingestion, ragweed pollen (RW) stimulate intestinal epithelial cells (IECs) to release chemoat-tractants (IL-6, IL-8, and MCP-1) that may increase the population of innate immune cells such as macrophages (MΦ) and dendritic cells (DCs) in the sub epithelial region. Subsequently, some RW may translocate to the underlying subepithelial region of the intestine. The exact mechanism behind RW translocation is still unknown ('?' symbol). Translocated RW can then interact with the resident immune cells or the newly recruited immune cells. RW interaction with DCs can lead to upregulation of activation and maturation molecules (CD40, CD80, CD86, and MHC-II). Additionally, RW can also activate macrophages. RW interaction with macrophages and DCs can stimulate release of inflammatory cytokines (IL-1β, TNF-α, IL-6), which can further help in the process of antigen presentation. The vaccine antigens can be carried in the cavity of the RW or in adsorbed form on the RW wall.